

Article

Countering Negative Effects of Terrain Slope on Airborne Laser Scanner Data Using Procrustean Transformation and Histogram Matching

Endre Hofstad Hansen *, Liviu Theodor Ene, Terje Gobakken, Hans Ole Ørka, Ole Martin Bollandsås and Erik Næsset

Faculty of Environmental Sciences and Natural Resource Management, Norwegian University of Life Sciences, P.O. Box 5003, NO-1432 Ås, Norway; eneliviu@gmail.com (L.T.E.); terje.gobakken@nmbu.no (T.G.); hans-ole.orka@nmbu.no (H.O.Ø.); ole.martin.bollandsas@nmbu.no (O.M.B.); erik.naesset@nmbu.no (E.N.)

* Correspondence: endre.hansen@nmbu.no

Received: 15 August 2017; Accepted: 16 October 2017; Published: 21 October 2017

Abstract: Forest attributes such as tree heights, diameter distribution, volumes, and biomass can be modeled utilizing the relationship between remotely sensed metrics as predictor variables, and measurements of forest attributes on the ground. The quality of the models relies on the actual relationship between the forest attributes and the remotely sensed metrics. The processing of airborne laser scanning (ALS) point clouds acquired under heterogeneous terrain conditions introduces a distortion of the three-dimensional shape and structure of the ALS data for tree crowns and thus errors in the derived metrics. In the present study, Procrustean transformation and histogram matching were proposed as a means of countering the distortion of the ALS data. The transformations were tested on a dataset consisting of 192 field plots of 250 m² in size located on a gradient from gentle to steep terrain slopes in western Norway. Regression models with predictor variables derived from (1) Procrustean transformed- and (2) histogram matched point clouds were compared to models with variables derived from untransformed point clouds. Models for timber volume, basal area, dominant height, Lorey's mean height, basal area weighted mean diameter, and number of stems were assessed. The results indicate that both (1) Procrustean transformation and (2) histogram matching can be used to counter crown distortion in ALS point clouds. Furthermore, both techniques are simple and can easily be implemented in the traditional processing chain of ALS metrics extraction.

Keywords: airborne laser scanning; histogram matching; steep terrain; point cloud; Procrustean transformation

1. Introduction

Airborne laser scanning (ALS) data have become an important source of auxiliary information to enhance forest inventories [1]. Forest attributes such as tree heights, diameter distributions, volumes, and biomass can be modeled utilizing the relationship between the metrics derived from remotely sensed data as predictor variables, and measurements of forest attributes on the ground. The quality of the models relies on the actual relationship between the forest attributes and the metrics derived from the remotely sensed data. Generally, these metrics can be described as “height” and “density” metrics providing proxies for the height and density of the forest canopy. For a more thorough description of the height and density metrics, see e.g., [2,3].

ALS systems work by scanning the area of interest and producing a three-dimensional cloud of point measurements. The elevation (z-value) of the point cloud is originally above sea level or above the ellipsoid. By constructing a digital terrain model (DTM), and subtracting the DTM elevation from the elevation of each of the points in the ALS data, a normalized point cloud is obtained.

Thus, the elevational values of the points in the normalized cloud are in height above the ground. The normalized point cloud constitutes a three-dimensional approximation of the vegetation above the ground surface. In areas with sloped terrain, the normalization process will introduce a “distortion” of the point clouds of individual tree crowns [4–6]. This distortion will influence the height and density metrics derived from the point cloud, depending on the terrain slope, tree species, and tree crown properties [5]. Such differences in the derived metrics caused by varying terrain slope conditions will weaken the relationship between forest attributes and metrics derived from the ALS data, resulting in poorer models in areas with sloped conditions and even for flat terrain if the models are constructed from data acquired under varying slope conditions. Furthermore, analyses of the relative importance of metrics used as predictor variables are frequently used to shed light on ecological relationships between organisms (e.g., [7,8]), or to enhance understanding of forest naturalness and evolution of canopy structure (e.g., [9]). These relationships may also be obscured by distorted point clouds.

Vega et al. [6] presented a solution to avoid some of the problems with crown distortion by first segmenting the individual trees using the untransformed ALS data, and thereafter normalizing the point clouds from each tree based on the DTM elevation at the coordinate of the tree apex. This approach was later used in steep terrain conditions in southern China [10]. However, identification of individual trees following this approach, known as the individual tree crown approach (ITC, [11]), generally requires high pulse density ALS data.

Unlike the ITC, the area-based approach (ABA, [12,13]) can be used for low pulse density ALS data. The collection of field and ALS data, and the subsequent data processing, modeling, and estimation of forest attributes usually follow a procedure described by Næsset [14] (p. 218–219). Due to data availability, costs, ease of implementation, and well-documented efficiency, the ABA has become the standard procedure for operational use of ALS to support forest inventories in the Nordic and many other countries [14,15].

In the present study, we explored and evaluated means of countering the negative effects of crown distortion within the ABA. To counter the effects of the normalization, the idea was to transform the normalized point cloud into the shape of the original point cloud, whilst preserving the elevational values in meters above the ground, and thus obtaining normalized point heights without deforming the shape of the point clouds of the tree crowns.

The transformation of a point cloud to another can be viewed as an orthogonal Procrustes problem. A least-square solution to a two-dimensional orthogonal Procrustes problem was first given by Boas [16], and later solved for any dimension by von Neumann [17]. Since then, the technique has developed further into the statistical field known as shape analysis or morphometrics [18,19], and is used in a range of research disciplines [20]. In our case, where the x and y coordinates of the two point clouds are identical, a simple least-square Procrustean transformation (PT) is sufficient for transforming the normalized point cloud into the shape of the original point cloud. In the current study, PT was adopted as a strategy to mitigate the effects of deformed point clouds.

Histogram matching (HM) is a common technique in image processing used to adjust color levels, normally gray, in one image to fit the distribution in another [21] (p. 94–97). Values of the attribute of interest in the dataset to be transformed, are adjusted to match the distribution in the target dataset. Because of its intuitive approach to transformation and ease of implementation, we selected HM as an alternative technique for transforming the normalized point clouds. Unlike PT, of which the authors have no knowledge of prior use in forestry, HM has been used for analysis of ALS data for estimation of forest attribute distributions. Ørka et al. [22] used HM for normalization of the intensity of ALS point clouds. Baffetta et al. [23] and Gilichinsky et al. [24] used HM to counter an averaging effect of the k-nearest neighbor’s technique. Vauhkonen and Mehtätalo [25] and Xu et al. [26] used HM and ITC to improve estimates of forest attributes, whilst Nyström et al. [27] used HM to calibrate distributions of metrics derived from multi-temporal ALS data. None of these studies, however used, HM to transform the actual ALS point clouds.

In the present study, both transformation methods were used to transform the normalized point cloud into the shape of the original point cloud. In addition to a transformation of the entire point cloud, different canopy thresholds were applied per plot to explore the effects of transforming only the part of the point clouds originating from the tree crowns. The reasoning behind the latter strategy was that the distortion from the normalization primarily affects the tree crowns.

To our knowledge, no studies have previously explored the possible effects of PT and HM as means to mitigate distortion of point clouds of tree crowns resulting from normalization of ALS data. The objectives of the present study were therefore to evaluate the effects of PT and HM on ALS metrics and forest attribute predictions by means of the standard procedures of the ABA. The effects of using metrics derived from transformed point clouds as predictor variables in regression models of six different forest attributes were compared to models with predictor variables derived from untransformed point clouds.

2. Materials and Methods

2.1. Study Area

The study area covered approximately 260 km² of productive forest, located on the west coast of Norway (60°10' N, 5°40' E, 0–500 m above sea level, Figure 1). The west coast of Norway is characterized by a diverse terrain of rugged mountains, fertile valleys, and a jagged coastline indented by fjords. The forest is naturally dominated by Scots pine (*Pinus sylvestris* L.) and deciduous species, mainly birch (*Betula pubescens* Ehrh.). However, planting of non-native conifers, mainly Norway spruce (*Picea abies* (L.) Karst.) and Sitka spruce (*Picea sitchensis* (Bong.) Carr.) became a prioritized area for public afforestation programs after the second World War and up to the 1970s. About 13% of the productive forest area is now covered by spruce [28]. The productive forest area contained terrain slope ranging up to 50° of inclination.

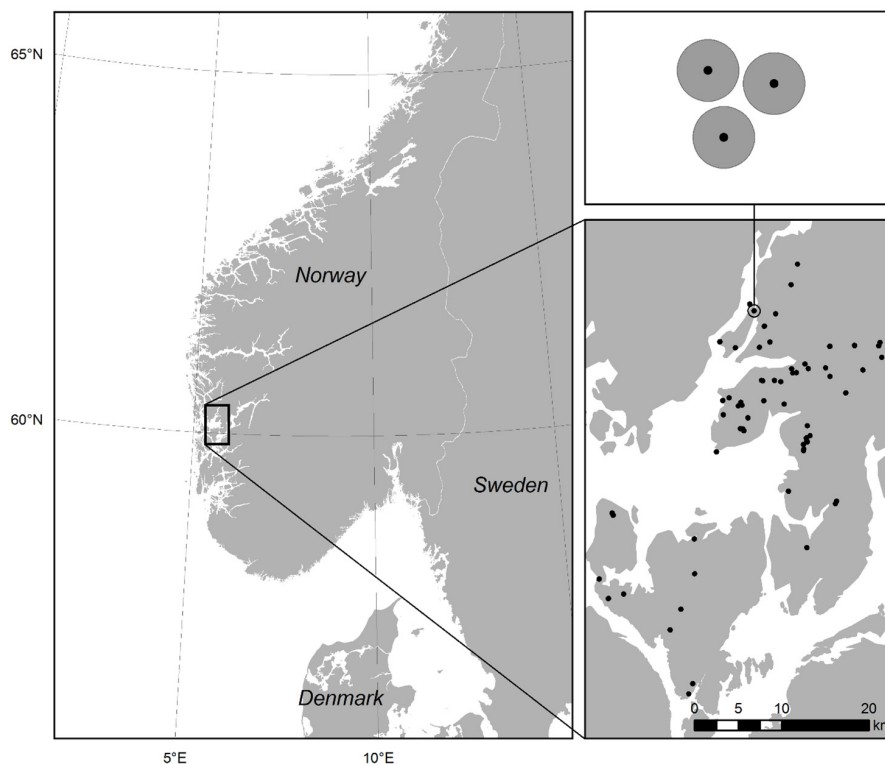


Figure 1. Map of the study area. Distribution of field sample clusters (lower right). Cluster design (top right).

2.2. Field Data

In total, 192 circular plots of 250 m² were established during the autumn of 2013. The plots were georeferenced using global navigation satellite systems (GNSS) (Global Positioning System (GPS) and global navigation satellite system (GLONASS)) with correction data from three of the official base stations of the Norwegian mapping authority closest to the study area. GNSS measurements were performed at two-second intervals for a minimum of 30 min. The accuracy of the coordinates was assessed by the estimated standard deviation of the post processing using the Pinnacle software [29]. The sample was initially designed to assess potential effects on estimation of forest attributes of terrain slope, sensor settings of the laser scanner, and tree species. Sample plots were therefore established in clusters of three and in a balanced experimental design with an equal number of plots covering five slope classes from zero to 50° of inclination and two dominating tree species classes: spruce and pine. Norway spruce (*P. abies*) dominated 68 of the spruce plots whilst 25 were dominated by Sitka spruce (*P. sitchensis*). The pine plots were dominated by Scots pine (*P. sylvestris*).

In each plot, species and diameter at breast height (DBH) were recorded for trees with DBH ≥ 4 cm. Three trees per plot (nine per cluster) were selected systematically for height measurement. An initial stem count was carried out to determine the stem number, after which every *n*'th tree was selected according to the stem number. For each of these sample trees, single tree volume was calculated using allometric models for birch [30], pine [31], spruce [32], and Sitka spruce [33]. Further, a base volume was calculated for the sample trees using an estimated height according to a base height model [34] and the observed DBH. Cluster- and species wise ratios were calculated between the mean “observed” volume of the sample trees and the corresponding mean base volume. These ratios were subsequently used as correction factors for the rest of the trees with no height measurements, by multiplying the ratio by the base volume of these trees. This estimator is known as the ratio-of-means estimator. If there were less than three sample trees of a certain species in a cluster, common species wise ratios calculated from the entire dataset were used as correction factors. Using the corrected volume estimates, heights of trees without height measurements were estimated with the appropriate single tree volume models [30–32]. Tree volumes were summarized on a plot level and scaled to per ha timber volumes (Vt) (Table 1). Dominant height (Hd), defined as the 100 largest trees per hectare according to DBH, and Lorey's mean height (Hl), i.e., mean height weighted by basal area, were calculated per plot from the estimated heights of all trees in the plots. In addition, other response variables at the plot level included basal area (G), basal area weighted mean diameter (Dg), and number of stems (Nt).

Table 1. Mean and standard deviation (in parenthesis) of forest attributes and ALS pulse density based on individual plots.

Dominant Species	Number of Sample Plots	Forest Attribute						Pulse Density (m ⁻²)
		Vt	G	Hd	Hl	Dg	Nt	
Pine	99	175.6 (82.2)	25.0 (9.4)	15.6 (2.3)	14.1 (2.5)	21.0 (5.6)	804 (427)	1.94 (0.76)
Spruce	93	591.8 (251.5)	56.5 (16.4)	25.1 (4.4)	21.4 (4.3)	23.1 (5.3)	1464 (587)	1.71 (0.93)
Total	192	377.2 (278.2)	40.2 (20.6)	20.2 (5.9)	17.7 (5.0)	22.0 (5.5)	1124 (607)	1.83 (0.85)

Vt = timber volume (m³ ha⁻¹), G = basal area (m² ha⁻¹), Hd = dominant height (m), Hl = Lorey's height (m), Dg = basal area weighted mean diameter (cm), Nt = number stems (*n* ha⁻¹).

2.3. ALS Data and Initial Processing

ALS data were acquired using two different Optech ALTM Gemini instruments mounted on PA31 Piper Navajo fixed-wing aircrafts during the period from 5 June to 7 August 2010. The sensors were flown at 1300 and 1600 m above ground level with an average speed of 80 ms⁻¹. The pulse repetition frequencies were 100 kHz and 70 kHz, with half scan angles of 12° and 19° and scan frequencies of 58 Hz and 41 Hz for the low and high altitude acquisitions, respectively. On average, the data had a pulse density of approximately two pulses m⁻². Following the acquisition, the contractor (Blom Geomatics AS, Oslo, Norway) performed initial processing. The processing of the point clouds followed a standard procedure of first creating a DTM and thereafter subtracting the elevation of the

DTM from the elevation of each ALS point resulting in an elevation above ground for the point cloud. The original point cloud before normalization is hereafter referred to as “Z”, and the normalized point cloud as “dZ”. The DTM was computed as a triangulated irregular network, and ground points were identified using the algorithm presented by Axelsson [35] using TerraScan software [36].

The Optech sensors provided records of up to five points per pulse. These points were categorized as “single”, “first of many”, “intermediate”, and “last of many” depending on their sequence of registration by the sensor system. Based on these categories the “first of many” and “single” points were merged into one dataset referred to as FIRST, and the “last of many” points constituted the LAST dataset.

2.4. Transformations

Two alternative transformation techniques—Procrustean transformation (PT) and histogram matching (HM) were used to counter the effect of the normalization. Details are provided in Sections 2.4.1 and 2.4.2 below.

The PT and HM were applied to: (1) the full *dZ* point cloud, and (2) the part of *dZ* above a height threshold separating points originating from the tree crowns. The reasoning behind the latter strategy was that the negative effect of the normalization affects mostly the tree crowns. The threshold in (2) was derived from the *dZ* as the minimum of the estimated kernel density distribution of ALS point heights (Figure 2). In cases where the distribution did not have a minimum in the range between the canopy top and the ground surface, the threshold was set to 1.3 m; a value commonly used to separate points originating from the tree crowns from ground vegetation (e.g., [37]). This resulted in five sets of point cloud data for further analysis:

- (1) the normalized point cloud (*dZ*),
- (2) the normalized point cloud with PT (*dZ.p*),
- (3) the normalized point cloud with PT above a threshold (*dZ.tp*),
- (4) the normalized point cloud with HM (*dZ.h*), and
- (5) the normalized point cloud with HM above a threshold (*dZ.th*).

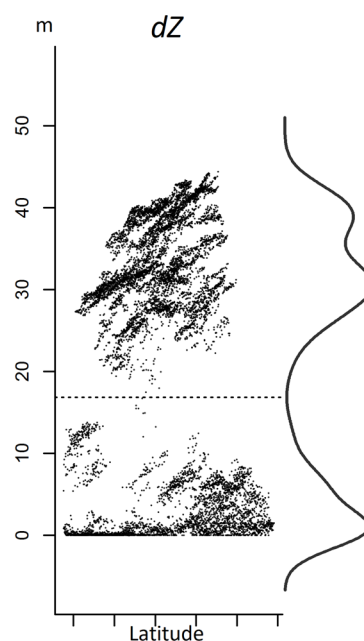


Figure 2. Visualization of the thresholding by finding the minimum (**dotted line**) of the estimated kernel density distribution (**solid line**) of the normalized point cloud (*dZ*).

2.4.1. PT

Procrustean analysis aims to find the optimal transformation for matching two matrix configurations—a ‘target’ matrix and a matrix to be transformed (or the ‘testee’), both matrices having the same dimensionality, such that the ‘testee’ would fit as close as possible to the ‘target’. In our case, the ‘target’ would be the untransformed ALS dataset, and the normalized ALS dataset is the ‘testee’. The ordinary PT result consists of a rotation matrix, a translation vector, and a scale parameter to be applied to the ‘testee’, such that the similarity differences between the ‘target’ and ‘testee’ are minimized according to the least-square criterion. The similarity measure between ‘target’ and ‘testee’ is defined as the Euclidean distances [38], ch. 7.1. The estimated parameters of PT are the result of an orthogonal least-squares solution. The main steps and the algebraic details for performing the Procrustean transformation are given in Borg and Groenen [39], pp. 430–432.

In our case, where we only look for adjusting the point heights, it is desirable that the point locations are not changed after transformation. It is also reasonable to assume that the point normalization process does not affect the scaling of the original data. For ease of use, the algorithm is also available in the R [40] packages “MCMCpack” [41], “vegan” [42], or “pracma” [43].

2.4.2. HM

The alternative technique used to transform the dZ into the shape of Z was HM. HM followed the procedure for continuous variables described in Gonzalez and Woods [21]. First, the empirical cumulative distribution of point elevation in both dZ and Z was computed (F_{dZ} and F_Z). Thereafter, the elevation of each point in dZ was adjusted to fit the height distribution in Z , using the quantile function (G) of the untransformed Z values as a mapping function (transformed $dZ = G[Z; F_{dZ}]$). In plain R [40] code, this can be formulated as:

$$\text{Transformed } dZ = \text{quantile}(Z, \text{probs} = \text{ecdf}(Z)(dZ)) \quad (1)$$

For the sole purpose of illustrating the different methods, a high pulse density ALS point cloud, covering a single tree with a wide crown growing in steep terrain, was used. The data were collected in a tropical rain forest in Amani Nature Reserve, Tanzania. A detailed description of the ALS data and the forest can be found in Hansen et al. [44]. The visualization of dZ clearly showed the deformation of the tree point cloud of the crown as an effect of the normalization process (Figure 3). Plots of $dZ.p$, $dZ.h$, and $dZ.th$ showed the effects of the applied transformations.

2.5. ALS Metrics

Height deciles (H1, H2, . . . , H9) were computed from points above or equal to a canopy threshold of 1.3 m. Measures of canopy density were computed by dividing the canopy height into ten equally large vertical intervals from the canopy threshold to the 95th height percentile as recommended by Næsset and Gobakken [45]. The proportion of points above each interval to the total number of points was computed, resulting in 10 density metrics D0, D1, . . . , D9. Furthermore, the mean height of points (Hmean) and coefficient of variation (Hcv) of the height were computed for points above the canopy threshold. The metrics were computed separately for each of the two datasets (i.e., FIRST and LAST), and a subscript F or L was used as notation. This resulted in 44 metrics derived from each of the ALS point cloud datasets (i.e., dZ , $dZ.p$, $dZ.tp$, $dZ.h$, and $dZ.th$).

Five metrics from the FIRST dataset (H8.F, Hmean.F, H2.F, D7.F, and D2.F) and the corresponding five metrics from the LAST dataset (H8.L, Hmean.L, H2.L, D7.L, and D2.L) were subjectively selected for visual examination. The selected metrics were chosen because they cover a sample of metrics frequently selected as predictor variables in previous studies (e.g., [45–47]).

These metrics were derived from dZ , $dZ.p$, and $dZ.h$ and they were used to examine the effects of the PT and HM. Scatter plots of each metric were produced by subtracting the value of each metric derived from each of the transformed point cloud datasets from the corresponding metric derived

from the dZ data. The changes in the metrics were plotted against terrain slope to visualize possible influences of terrain slope. Linear models of terrain slope regressed against the changes in the metrics were also fitted. A significant slope of the regression line indicated that the metric had been changed as a result of terrain slope. This test of the effect of slope on the change in ALS-derived metrics could be confused by correlations between the forest height and terrain slope. It is possible to envisage a situation where the change in a selected metric is simply an effect of the height of the trees, where the metric describing a forest with large trees will have large changes as an effect of the transformation, and the same metric from a forest with smaller trees will have smaller changes. To assess any such potential effects on the significance of the terrain slope we computed and evaluated the correlation between Hmean.F and terrain slope. We found the correlation to be small (0.17), and thus the effect of slope on the change in ALS-derived metrics should not be confused by correlations between the forest height and terrain slope.

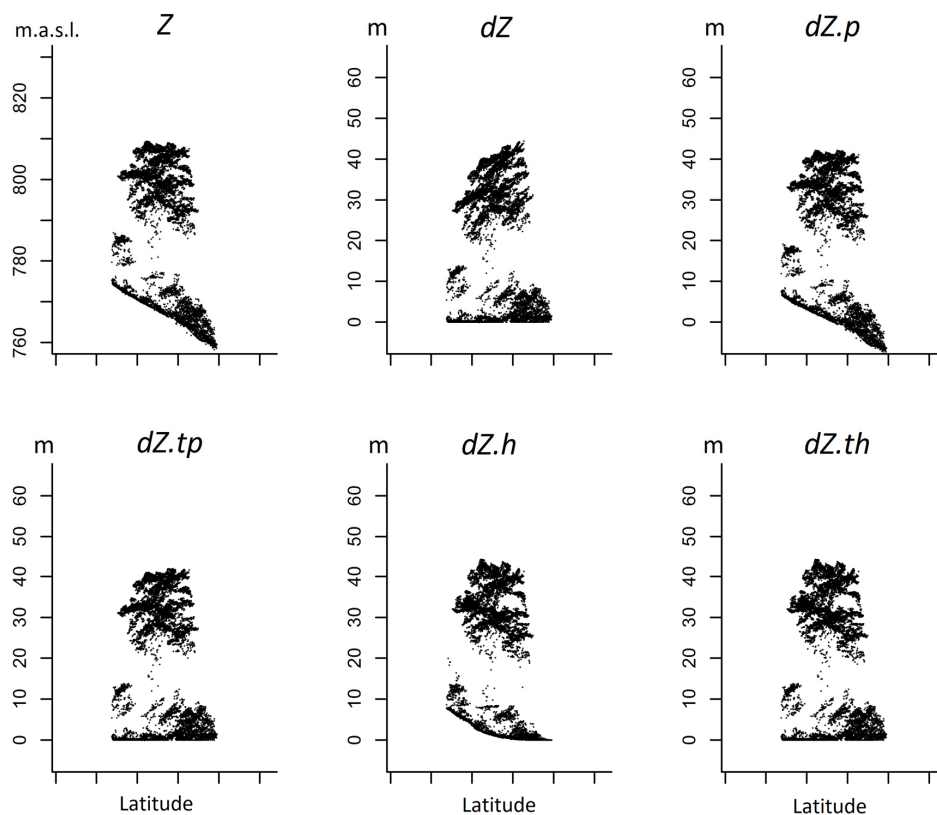


Figure 3. Visualization of point clouds from a single tree in Amani Nature Reserve, Tanzania. The graphical panel shows the original point cloud before normalization (Z), normalized point cloud (dZ), Procrustean transformed point cloud ($dZ.p$), Procrustean transformed point cloud with threshold ($dZ.tp$), histogram matched point cloud ($dZ.h$), and histogram matched point cloud with threshold ($dZ.th$).

2.6. Generalized Linear Modeling

Practical applications of ABA forest inventory assisted by ALS data often applies stratification to improve estimation (e.g., [47]). We, therefore, stratified the data in the present study into two strata according to dominant species prior to modelling. The strata were denoted spruce and pine. The following modelling procedures were thus performed for the two strata separately.

The 44 metrics derived from the ALS data were used as candidate predictor variables. With such a large number of candidate variables, an initial selection of variables was necessary to avoid computational problems in the subsequent model fitting procedure. Thus, an initial model containing

25 variables was selected based on the Akaike information criterion with correction for finite samples (AICc, [48]) implemented in the FWDselect package [49] in R [40]. The model was defined as a generalized linear model (GLM) with a square-root link function and assuming a gamma distribution of the response variables. The gamma distribution was chosen based on the positive distribution of the response variables as described in Zuur et al. [50]. Moreover, the gamma distribution assumes a functional relationship between mean and variance, making it suitable for situations with heteroskedastic errors. Further, the 25 variables from the initial model were used as candidate variables in a best subset selection procedure implemented in the glmulti package [51]. This procedure was set to report GLM models of up to three predictor variables ranked by AICc. Then, the best model according to the AICc and with a variation inflation factor (VIF) of less than three was chosen as the prediction model for each of the six response variables. Finally, a five-fold cross validation of the selected models was incorporated, and the cross validated mean absolute error (MAE) and root mean square error (RMSE) were used as two complementary evaluation criteria as recommended by Chai and Draxler [52].

2.7. Summarizing Modeling Results

The cross validation resulted in model errors (i.e., MAE and RMSE) for each of the five point clouds, for the six forest attributes, and for the two strata. To summarize the effects of the transformations and use of each of the five point clouds on the model errors for all forest attributes, an overall score was computed. The score indicated if the applied point clouds resulted in a reduced overall error for the six forest attributes. The score was calculated for the two strata separately as:

$$OS_i = \sum_{j=1}^J \frac{E_{ij} - D_j}{D_j}, \quad (2)$$

where OS_i is the overall score for point cloud $i = 1, 2, \dots, 5$, j is the forest attribute ($j = 1, 2, \dots, J = 6$), E_{ij} is the sum of MAE_{ij} and $RMSE_{ij}$ resulting from point cloud i for attribute j , and D_j is the sum of MAE_j and $RMSE_j$ resulting from dZ for forest attribute j . For dZ , the score will be zero. A negative score indicates that the transformation technique resulted in model errors smaller than those resulting from the dZ .

3. Results

3.1. ALS Metrics

The effects of the transformations on the selected ALS metrics were visualized by means of graphical plots showing the changes in the ALS metrics against terrain slope (Figures 4–7). The changes were calculated as the value of each metric derived from the transformed point clouds minus the value of the corresponding metric derived from dZ . The plots also included a linear fit of terrain slope to the change for each metric, accompanied by a significance level of the slope of the linear fit.

For PT, scatter plots of changes in the metrics derived from the FIRST dataset showed that changes increased with increasing terrain slope (Figure 4). For the height metric from the top half of the canopy (H8.F), the changes were positive, i.e., the $dZ.p$ value increased relative to dZ with terrain slope. The transformation increased H8.F by approximately 0.6 m on the steepest terrain. For the ALS metric characterizing the lower part of the canopy (H2.F), PT had the opposite effect ($p < 0.001$) with decreasing values with increasing terrain slope. The effects of PT on the mean canopy height were moderate, with a decreased mean height of 0.2 m on the steepest slopes for pine. For spruce, there was no significant correlation between terrain slope and changes in mean canopy height (Figure 4). Both density metrics (D7.F and D2.F) for both species showed a negative change as the terrain slope increased.

The effect of PT on metrics derived from the LAST dataset showed similar effects of the transformed point heights as the metrics derived from the FIRST dataset (Figure 5). The effects

were, however, attenuated. Only H8.L, H2.L, and D7.L from the spruce plots, and D2.L from the pine plots showed significant changes related to terrain slope ($p < 0.05$).

For HM, the effect on the metrics derived from the FIRST dataset also showed changes with terrain slope (Figure 6). Metric values were reduced with increasing slope for all metrics except for H8.F in spruce plots. Attention can be drawn to scatter plots of the changes in Hmean.F, showing a reduction in mean pulse height of 1.7 and 0.4 m for pine and spruce, respectively. The effects of HM on metrics derived from the LAST dataset were similar to those from the PT.

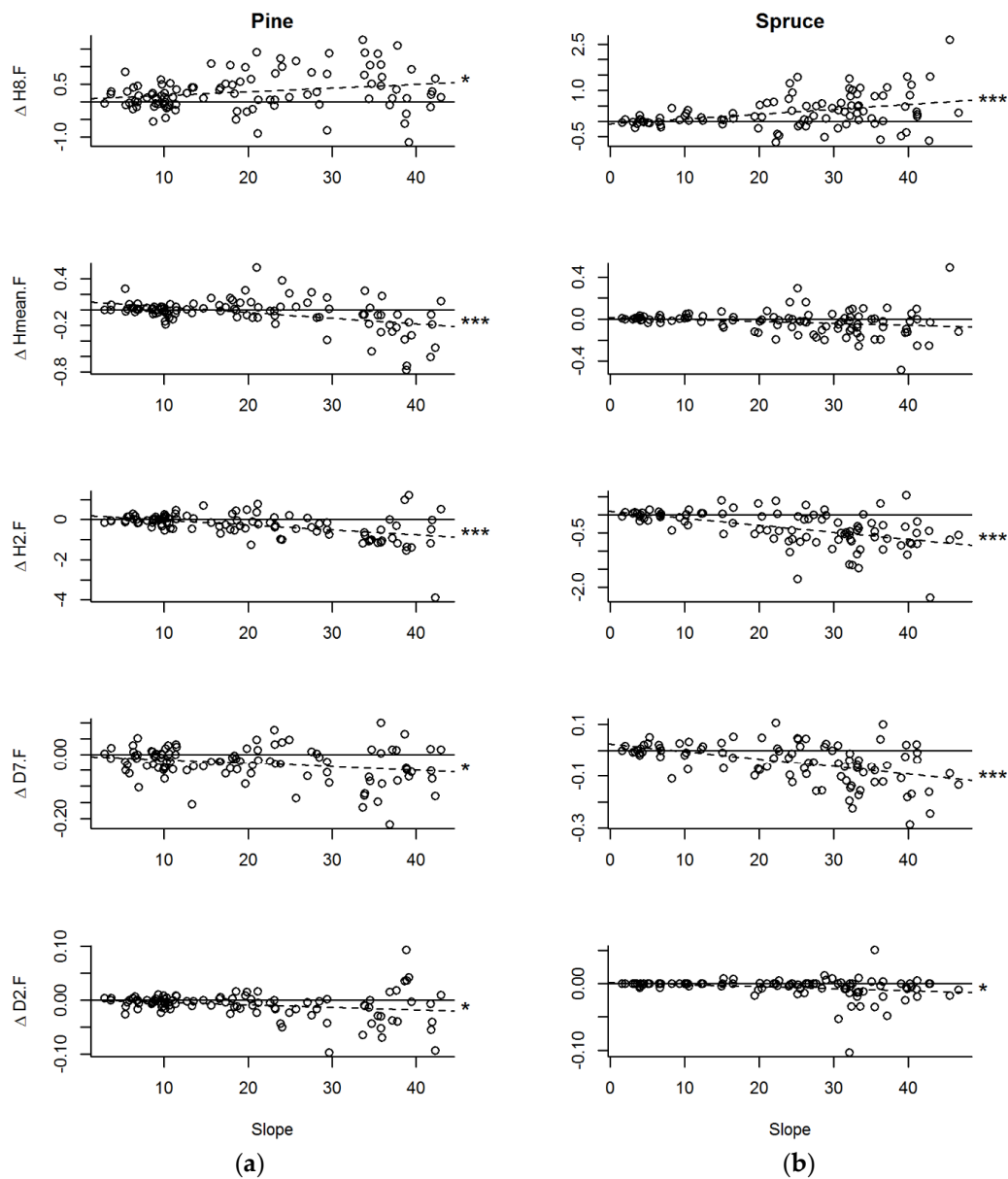


Figure 4. Effect of Procrustean transformation on five ALS metrics of the FIRST return category (H8.F, Hmean.F, H2.F, D7.F, and D2.F). The change in metric value (Δ) is plotted against terrain slope for the pine stratum (a) and spruce stratum (b). Solid line = 0.0 line, dashed line = linear fit. Significance of linear fit: *** $p < 0.001$, * $p < 0.05$.

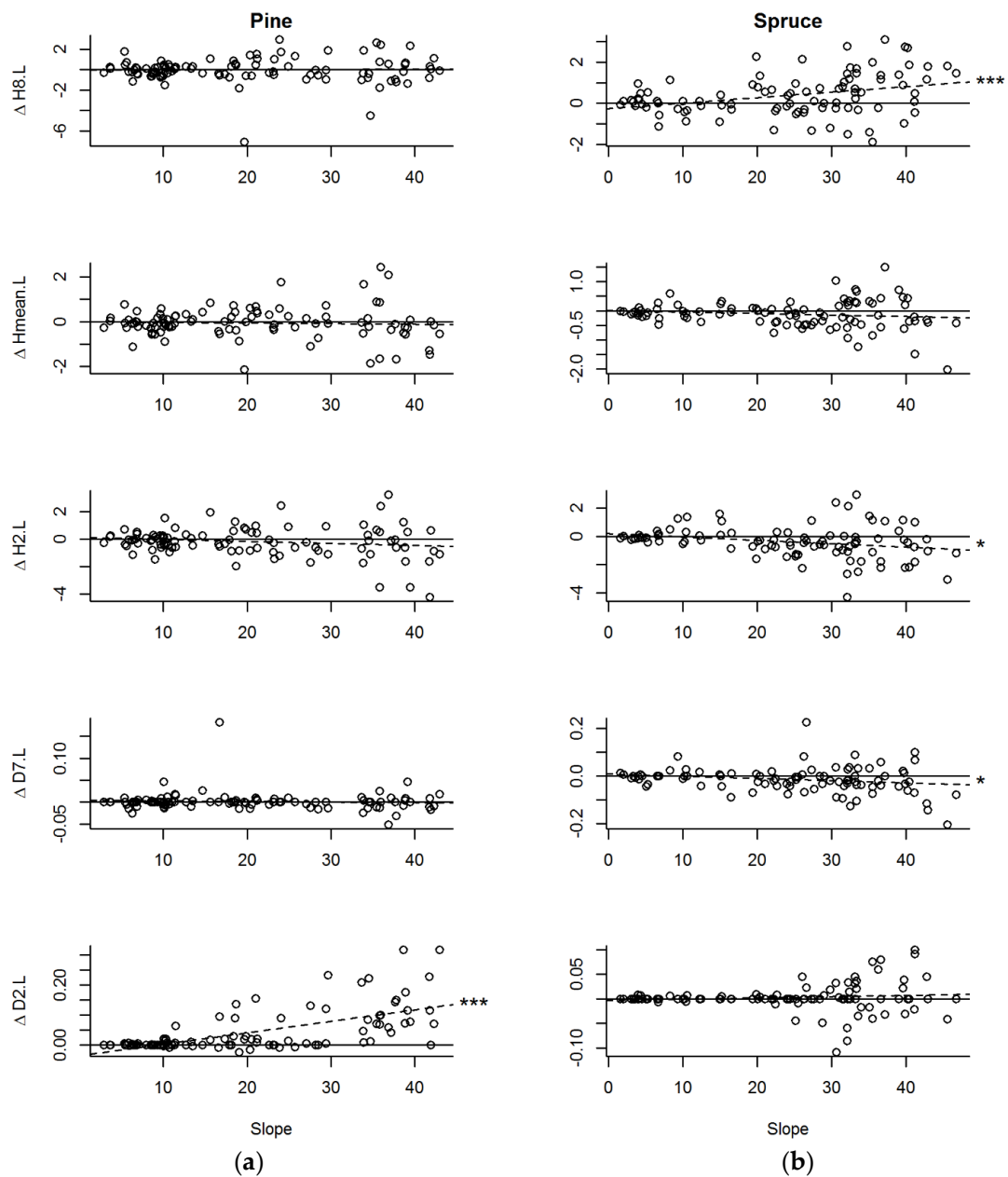


Figure 5. Effect of Procrustean transformation on five ALS metrics of the LAST return category (H8.L, Hmean.L, H2.L, D7.L, and D2.L). The change in metric value (Δ) is plotted against terrain slope for the pine stratum (a) and spruce stratum (b). Solid line = 0.0 line, dashed line = linear fit. Significance of linear fit: *** $p < 0.001$, * $p < 0.05$.

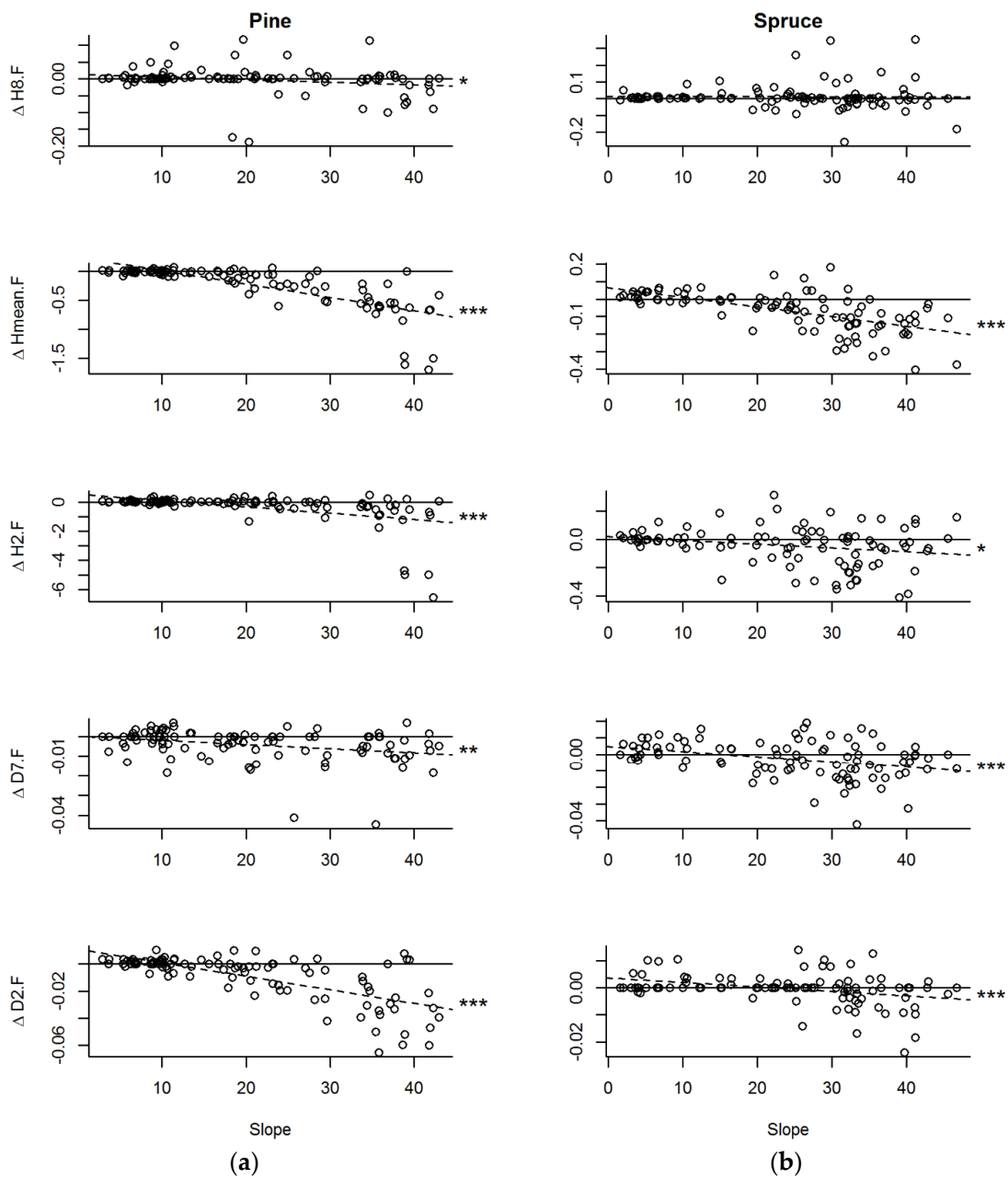


Figure 6. Effect of histogram matching on five ALS metrics of the FIRST return category (H8.F, Hmean.F, H2.F, D7.F, and D2.F). The change in metric value (Δ) is plotted against terrain slope for the pine stratum (a) and spruce stratum (b). Solid line = 0.0 line, dashed line = linear fit. Significance of linear fit: *** $p < 0.001$, ** $p < 0.01$, * $p < 0.05$.

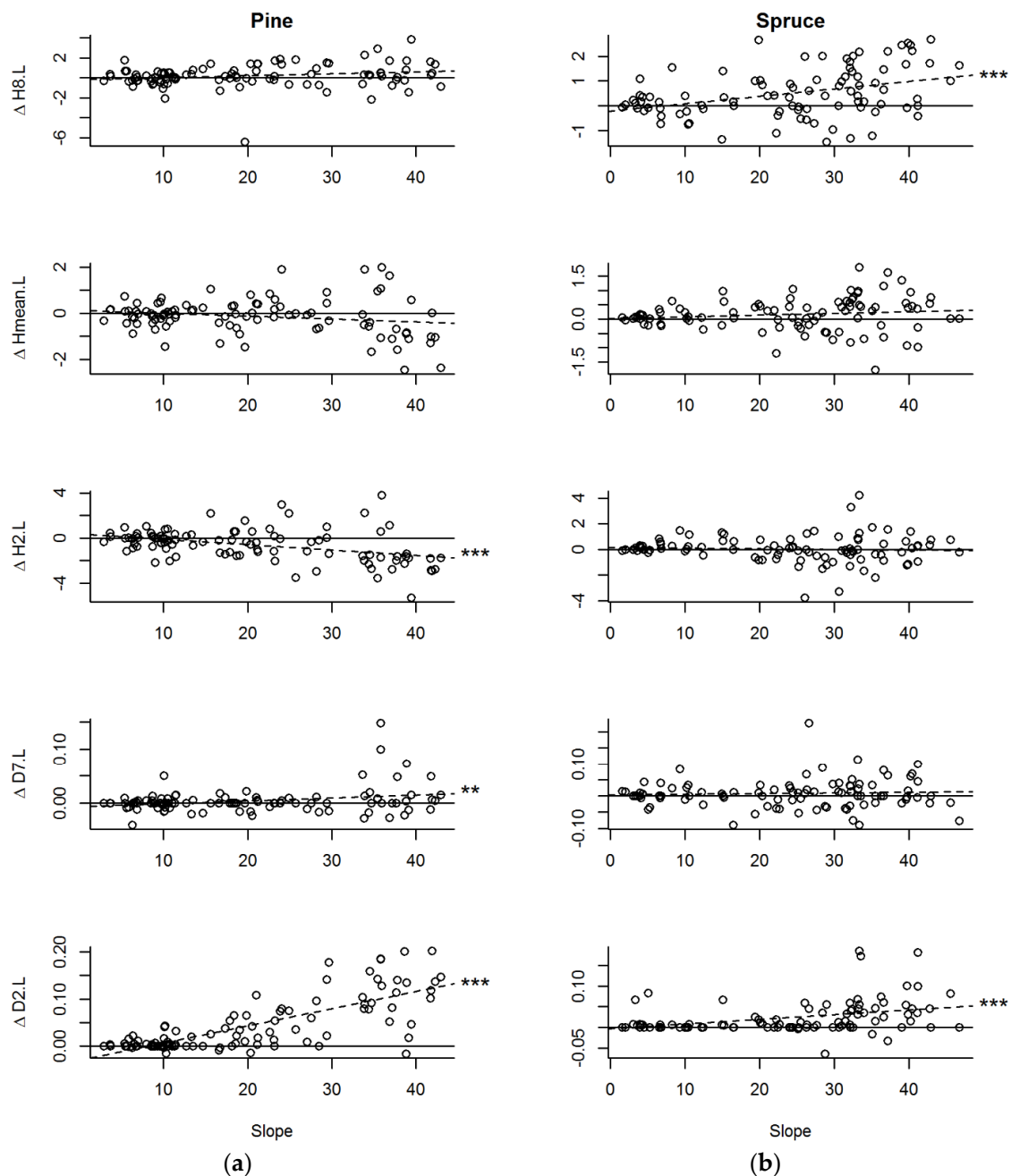


Figure 7. Effect of histogram matching on five ALS metrics of the LAST return category (H8.L, Hmean.L, H2.L, D7.L, and D2.L). The change in metric value (Δ) is plotted against terrain slope for the pine stratum (a) and spruce stratum (b). Solid line = 0.0 line, dashed line = linear fit. Significance of linear fit: *** $p < 0.001$, ** $p < 0.01$.

3.2. Regression Models

GLM models were fitted separately for the five response variables of interest: Vt, G, Hd, Hl, Dg, and Nt, and for the two strata based on dominant species, pine, and spruce. Furthermore, metrics derived from the five point clouds, dZ , $dZ.p$, $dZ.tp$, $dZ.h$, and $dZ.th$, were used separately as predictor variables.

The assessment of the forest attribute models based on the transformed point clouds using the two evaluation criteria (MAE and RMSE) showed smaller errors than the untransformed data (Tables 1 and 2). The positive effect of transformation was most pronounced for the pine stratum (Table 2),

for which models for all responses showed reduced MAE and RMSE values when transformed point clouds were used. Models based on variables derived from *dZ.h* resulted in reduced RMSE of 9.1%, 4.9%, and 7.2% for Vt, G, and Hl, respectively (Table 2). HM with threshold also performed well for modelling some of the forest attributes. The MAE and RMSE values of the Dg models were reduced by 11.3% and 8.0%, respectively.

For the spruce stratum as well, the models fitted with variables derived from transformed point clouds generally had smaller MAE and RMSE values compared to the models with variables derived from *dZ* (Table 3). The reduction in MAE and RMSE was, however, smaller than the reduction found for the pine stratum. For G and Dg, the transformations were not found to generally improve the models. The largest effect in terms of reduced MAE and RMSE was found for Hd and Nt, for which the transformation consistently reduced the errors (Table 3). The metrics selected as predictor variables in the models based on transformed data were different from the *dZ* models for all forest attributes (Tables 2 and 3).

Table 2. Summary of modelling results from five point clouds (*dZ*, *dZ.p*, *dZ.tp*, *dZ.h*, and *dZ.th*) for the pine stratum.

Point Cloud	Response	Predictor Variables	MAE*	RMSE*
<i>dZ</i>	G	D6.F, H2.L	5.61	6.98
<i>dZ.p</i>	G	H1.F, D5.F, D4.L	5.39	7.22
<i>dZ.tp</i>	G	H1.F, D7.F, D1.L	5.49	7.32
<i>dZ.h</i>	G	D6.F, H1.L, D9.L	5.30	6.64
<i>dZ.th</i>	G	D6.F, H3.L, D9.L	5.90	7.49
<i>dZ</i>	Dg	Hcv.F, H6.F, D2.F	3.42	4.31
<i>dZ.p</i>	Dg	H6.F, D2.L, D8.L	3.38	4.21
<i>dZ.tp</i>	Dg	Hmax.F, H4.F, D1.F	3.65	4.72
<i>dZ.h</i>	Dg	H6.F, D1.L, D8.L	3.27	4.25
<i>dZ.th</i>	Dg	H6.F, D1.L, D9.L	3.04	3.96
<i>dZ</i>	Hl	H5.F, D9.F, H7.L	1.27	1.63
<i>dZ.p</i>	Hl	H4.F, D9.F	1.31	1.65
<i>dZ.tp</i>	Hl	H4.F, D9.F	1.27	1.62
<i>dZ.h</i>	Hl	H5.F, D9.F	1.19	1.52
<i>dZ.th</i>	Hl	Hcv.F, H5.F, D9.F	1.30	1.65
<i>dZ</i>	Hd	Hcv.F, H7.F, D9.F	1.28	1.67
<i>dZ.p</i>	Hd	Hcv.F, H6.F, D9.F	1.25	1.62
<i>dZ.tp</i>	Hd	Hcv.F, H8.F, D9.L	1.27	1.64
<i>dZ.h</i>	Hd	H50.F, D9.F	1.29	1.63
<i>dZ.th</i>	Hd	Hcv.F, H8.F, D9.F	1.25	1.65
<i>dZ</i>	Nt	H7.F, D1.F, D1.L	272.8	371.4
<i>dZ.p</i>	Nt	H6.F, D3.F, D4.L	272.1	364.1
<i>dZ.tp</i>	Nt	H6.F, D1.F, D3.L	276.5	363.2
<i>dZ.h</i>	Nt	H5.F, D0.F, D1.L	277.7	374.3
<i>dZ.th</i>	Nt	H5.F, D7.F, D1.L	273.9	367.7
<i>dZ</i>	Vt	H1.F, D7.F, H2.L	42.4	56.9
<i>dZ.p</i>	Vt	H2.F, D7.F, D4.L	43.9	59.0
<i>dZ.tp</i>	Vt	H3.F, D7.F, D4.L	44.2	59.8
<i>dZ.h</i>	Vt	H6.F, D7.F, H1.L	38.9	51.7
<i>dZ.th</i>	Vt	H2.F, D7.F, D9.L	42.0	54.9

G = basal area, Dg = basal area weighted mean diameter, Hl = Lorey's mean height (Hl), Hd = dominant height, Nt = number of stems, Vt = timber volume. MAE = mean absolute error from cross validation. RMSE = root mean square error from cross validation. Smallest errors for each response variable highlighted in grey. * Units in $\text{m}^2 \text{ha}^{-1}$ for G, m for Hd and Hl, cm for Dg, n ha^{-1} for Nt, and $\text{m}^3 \text{ha}^{-1}$ for Vt).

Table 3. Summary of modelling results from the five point clouds (*dZ*, *dZ.p*, *dZ.tp*, *dZ.h*, and *dZ.th*) for the spruce stratum.

Point Cloud	Response	Predictor Variables	MAE*	RMSE*
<i>dZ</i>	G	Hmax.F, Hcv.F	10.98	14.17
<i>dZ.p</i>	G	H1.F, D0.F, D7.L	11.36	13.95
<i>dZ.tp</i>	G	Hcv.F, H9.F	11.64	14.70
<i>dZ.h</i>	G	Hmax.F, Hcv.F	11.43	14.00
<i>dZ.th</i>	G	Hmax.F, Hcv.F, D8.L	11.14	14.09
<i>dZ</i>	Dg	Hcv.F, H9.F, D9.L	2.76	3.65
<i>dZ.p</i>	Dg	H8.F, D9.F, D9.L	2.92	3.70
<i>dZ.tp</i>	Dg	H1.F, H8.L, D7.L	2.89	3.87
<i>dZ.h</i>	Dg	H8.F, D7.F, H1.L	2.79	3.75
<i>dZ.th</i>	Dg	H1.F, H9.F, D8.L	2.92	3.72
<i>dZ</i>	Hl	H9.F, D0.L	1.69	2.09
<i>dZ.p</i>	Hl	H1.F, H8.F, D8.L	1.71	2.04
<i>dZ.tp</i>	Hl	H9.F, D8.L	1.64	2.09
<i>dZ.h</i>	Hl	H8.F, D1.F, D5.F	1.78	2.15
<i>dZ.th</i>	Hl	H8.F, D0.F, D4.F	1.75	2.13
<i>dZ</i>	Hd	H6.F, D0.F, D6.F	1.86	2.33
<i>dZ.p</i>	Hd	H8.F, D8.L	1.77	2.20
<i>dZ.tp</i>	Hd	H9.F, D2.F	1.71	2.19
<i>dZ.h</i>	Hd	H8.F, D1.F, D5.F	1.80	2.25
<i>dZ.th</i>	Hd	Hmean.F, D0.F, D5.F	1.79	2.24
<i>dZ</i>	Nt	H1.F, H9.L, D9.L	340.2	447.8
<i>dZ.p</i>	Nt	H1.F, H7.L, D2.L	338.5	435.9
<i>dZ.tp</i>	Nt	H1.F, H8.L	329.5	421.3
<i>dZ.h</i>	Nt	D2.F, H9.L, D1.L	324.0	404.5
<i>dZ.th</i>	Nt	H2.F, H9.L, D3.L	340.8	427.1
<i>dZ</i>	Vt	Hmax.F, H1.F	124.7	174.4
<i>dZ.p</i>	Vt	Hmean.F, D0.F, D8.L	134.6	184.4
<i>dZ.tp</i>	Vt	Hcv.F, H9.F, D8.L	124.1	172.4
<i>dZ.h</i>	Vt	Hmax.F, H1.F, D8.L	125.9	178.1
<i>dZ.th</i>	Vt	Hmax.F, H1.F, D8.L	121.8	169.7

G = basal area, Dg = basal area weighted mean diameter, Hl = Lorey's mean height (Hl), Hd = dominant height, Nt = number of stems, Vt = timber volume. MAE = mean absolute error from cross validation. RMSE = root mean square error from cross validation. Smallest errors for each response variable highlighted in grey. * Units in $\text{m}^2 \text{ha}^{-1}$ for G, m for Hd and Hl, cm for Dg, n ha^{-1} for Nt, and $\text{m}^3 \text{ha}^{-1}$ for Vt).

3.3. Summarizing Modeling Results

The results of modelling errors were summarized for each point cloud as an overall score (OS, Equation (1)) for each stratum. For the pine stratum, the OS value showed that use of the *dZ.h* resulted in the smallest errors (OS = -0.24). The other point clouds resulted in OS values of -0.06 , -0.01 , and 0.12 for *dZ.th*, *dZ.p*, and *dZ.tp*, respectively. For the spruce stratum, all point clouds resulted in almost identical OS values with -0.03 , -0.02 , -0.02 , and 0.03 for *dZ.tp*, *dZ.h*, *dZ.th*, and *dZ.p*, respectively. In summary, the *dZ.h* resulted in an OS value indicating that HM transformation reduces the model errors most relative to the other transformations we evaluated.

4. Discussion

PT and HM were applied to mitigate the distortion of ALS point heights introduced during the height normalization process. The transformations were easy to implement and fast to perform using common, open source statistical and data processing software [40], which is an asset in operational implementation.

The effects of the transformations on the low point density data from western Norway were first assessed by inspecting the ALS metrics directly. Scatterplots of the changes in metric values from *dZ* to *dZ.p* and *dZ.h* showed the effects of the transformations (Figures 4–7). The plots also showed

that terrain slope had varying effects on the change in metric values. Metrics derived from the FIRST dataset were most affected by the transformations. Furthermore, except for H8.F derived from PT point clouds, the numerical values were reduced for most of these metrics as a result of the transformation. The metric values derived from the transformed point clouds were increasingly smaller with increased terrain slope, compared to those derived from dZ .

For trees growing on sloped terrain, the downhill part of tree crowns constitutes the largest portion of the total tree crown. The changes in the derived metrics indicate that the transformation reduces the height of the downward facing part of the crown and increases the upward facing part. Since the downward facing part is larger than the upward facing, the effect of the transformation is greater for the downward facing part, resulting in reduced metric values. This finding concurs with Breidenbach et al. [2], who stated that the height of ALS point clouds from trees growing on steep slopes would be overestimated because of the imbalance of crown size on upward and downward facing slopes. Because we applied the transformations on a plot level instead of a single tree level, this effect is reduced to the transformation of the crown of trees along the edge of the plots, leaving the trees in the middle of the plot less affected.

HM had a stronger effect on the mean height of the point clouds (Figure 6) compared to PT. The change in Hmean.F was significant and negative for both strata (pine and spruce). The mean height is often among the variables most strongly correlated to V_t and G , and this observation is therefore of great interest as it is often used as a single variable in modelling forest attributes, such as biomass [53]. Metrics derived from the LAST dataset were less affected by the transformations (Figures 5 and 7), and seem to be less influenced by terrain slope than the variables from the FIRST dataset. The cause of the difference in effect on metrics from the FIRST and LAST datasets is explained by the fact that the FIRST points describe the surface of the canopy and the shape of tree crowns. The LAST points generally stem from lower parts of the canopy and are therefore less affected by the transformation.

The regression modelling generally showed improved models using metrics derived from the transformed point clouds as predictor variables. Models for the pine stratum produced smaller errors than for the spruce stratum. For the pine stratum, the models were improved for all response variables when metrics derived from transformed point clouds were used. Using metrics derived from $dZ.h$ reduced the RMSE and MAE for V_t by 9.1% and 8.4%, respectively. For the spruce stratum, the effects of the transformations were less pronounced. Models for G and D_g were generally better using dZ . For the V_t -models, the RMSE and MAE values were reduced by 2.7% and 2.3%, respectively. The largest improvement in RMSE and MAE in the spruce stratum was found for H_d , for which transformations consistently improved the models. The stronger results of transformations in pine compared to spruce was as expected as we anticipated larger effects of the transformations for the wider pine crowns, coherent with the findings in Khosravipour et al. [3].

The calculated OS summarized the relative modelling error of using various transformations. For the pine stratum, models using the $dZ.h$ resulted in smaller errors compared to using other point clouds. For pine, the OS was similar for all point clouds, indicating that the point clouds result in equal model errors. Overall, the $dZ.h$ reduced the errors for pine models and did not increase errors for spruce models. The applied threshold in the transformation did not reduce the model errors. This suggests that properties from the higher parts of the point clouds of tree crowns are more important in modelling forest attributes compared to the lower parts. This is in line with previous research. Models for several forest properties constructed by Næsset [46] showed that height variables often are selected from the top three deciles.

Even though the proposed transformation showed positive results for ABA, it is logical to extend the Procrustes transformation to other forestry-related applications for which the positive effects of the transformation could be even stronger. For instance, the edge tree correction approach proposed by Packalen et al. [54] uses tree crown identification to aid the determination of which tree crowns belong to trees inside the field plot. This technique relies on a correct identification of tree crowns

and their location, both of which are disrupted in sloped areas as shown in Khosravipour et al. [3]. The semi-individual tree crown (SITC) approach described by Breidenbach et al. [55] and other ITC approaches (e.g., [11]) are affected similarly. Furthermore, the proposed transformation could be relevant for data similar in structure to the ALS data such as image matching [56,57] or single photon-counting laser instruments [58,59]. Under high pulse density conditions suitable for ITC approaches, the transformations should be assessed as a means of countering crown distortions for single trees. This should improve both the tree positioning and yield more accurate tree level metrics.

The current study is, to the very best of our knowledge, the first attempt to explore the use of PT and HM for countering the negative effects of crown distortion caused by normalization. The discussion in the preceding paragraph suggests that there are many modelling techniques (i.e., ABA, ABA with edge tree correction, ITC, SITC) and remotely sensed data (i.e., image matching, single photon-counting lasers) for which the proposed transformations would be relevant for further research.

5. Conclusions

The normalization process of ALS point clouds from vegetated areas on sloped terrain introduces a distortion of the point cloud heights. This distortion affects the information (i.e., the ALS metrics) derived from the point cloud on both a tree and area level. From the present study, we conclude that the proposed transformations are promising techniques for countering the negative effects of working with distorted ALS point clouds in forestry-related applications. The transformations could improve the analytical significance of ALS-derived metrics as well as the modelling of forest attributes. Following an ABA to modelling forest attributes, models for pine from transformed point clouds reduced the errors in three fifths of the GLM models. For spruce, there were only small effects of the transformations. Overall, HM transformation reduced the model errors for pine forest attributes while the model errors for spruce forest attributes did not increase. We, therefore, recommend HM for use in modelling forest attributes under the ABA. Furthermore, it is likely that even ITC approaches based on single tree point clouds would benefit from the proposed transformations. This should, however, be subject to further studies.

Acknowledgments: We wish to thank Vestskog B.A. for carrying out the field work. The study was funded by the Research Council of Norway as part of the project entitled “Sustainable Utilization of Forest Resources in Norway” (grant #225329/E40).

Author Contributions: E.H.H. and L.T.E. conceived and designed the experiments; E.H.H. performed the experiments; T.G., H.O.Ø., O.M.B., and E.N. contributed materials. E.H.H. wrote the paper with contributions from all co-authors through the editorial process.

Conflicts of Interest: The authors declare no conflict of interest.

References

1. White, J.C.; Coops, N.C.; Wulder, M.A.; Vastaranta, M.; Hilker, T.; Tompalski, P. Remote sensing technologies for enhancing forest inventories: A review. *Can. J. Remote Sens.* **2016**, *42*, 619–642. [[CrossRef](#)]
2. Bollandsås, O.M.; Hanssen, K.H.; Marthiniussen, S.; Næsset, E. Measures of spatial forest structure derived from airborne laser data are associated with natural regeneration patterns in an uneven-aged spruce forest. *For. Ecol. Manag.* **2008**, *255*, 953–961. [[CrossRef](#)]
3. Breidenbach, J.; Astrup, R. The Semi-Individual Tree Crown Approach. In *Forestry Applications of Airborne Laser Scanning*; Maltamo, M., Næsset, E., Vauhkonen, J., Eds.; Springer Science Business Media: Dordrecht, The Netherlands, 2014; pp. 113–133.
4. Breidenbach, J.; Koch, B.; Kändler, G.; Kleusberg, A. Quantifying the influence of slope, aspect, crown shape and stem density on the estimation of tree height at plot level using lidar and InSAR data. *Int. J. Remote Sens.* **2008**, *29*, 1511–1536. [[CrossRef](#)]
5. Khosravipour, A.; Skidmore, A.K.; Wang, T.; Isenburg, M.; Khoshelham, K. Effect of slope on treetop detection using a LiDAR Canopy Height Model. *ISPRS J. Photogramm. Remote Sens.* **2015**, *104*, 44–52. [[CrossRef](#)]

6. Vega, C.; Hamrouni, A.; El Mokhtari, S.; Morel, J.; Bock, J.; Renaud, J.P.; Bouvier, M.; Durrieu, S. PTrees: A point-based approach to forest tree extraction from lidar data. *Int. J. Appl. Earth Obs. Geoinf.* **2014**, *33*, 98–108. [[CrossRef](#)]
7. Graf, R.F.; Mathys, L.; Bollmann, K. Habitat assessment for forest dwelling species using LiDAR remote sensing: Capercaillie in the Alps. *For. Ecol. Manag.* **2009**, *257*, 160–167. [[CrossRef](#)]
8. Hill, R.A.; Hinsley, S.A. Airborne lidar for woodland habitat quality monitoring: Exploring the significance of lidar data characteristics when modelling organism-habitat relationships. *Remote Sens.* **2015**, *7*, 3446–3466. [[CrossRef](#)]
9. Sverdrup-Thygeson, A.; Ørka, H.O.; Gobakken, T.; Næsset, E. Can airborne laser scanning assist in mapping and monitoring natural forests? *For. Ecol. Manag.* **2016**, *369*, 116–125. [[CrossRef](#)]
10. Duan, Z.; Zhao, D.; Zeng, Y.; Zhao, Y.; Wu, B.; Zhu, J. Assessing and Correcting Topographic Effects on Forest Canopy Height Retrieval Using Airborne LiDAR Data. *Sensors* **2015**, *15*, 12133–12155. [[CrossRef](#)] [[PubMed](#)]
11. Hyypä, J.; Inkinen, M. Detecting and estimating attributes for single trees using laser scanner. *Photogramm. J. Finl.* **1999**, *16*, 27–42.
12. Næsset, E. Determination of mean tree height of forest stands using airborne laser scanner data. *ISPRS J. Photogramm. Remote Sens.* **1997**, *52*, 49–56. [[CrossRef](#)]
13. Næsset, E. Estimating timber volume of forest stands using airborne laser scanner data. *Remote Sens. Environ.* **1997**, *61*, 246–253. [[CrossRef](#)]
14. Næsset, E. Area-Based Inventory in Norway—From Innovation to an Operational Reality. In *Forestry Applications of Airborne Laser Scanning*; Maltamo, M., Næsset, E., Vauhkonen, J., Eds.; Springer Science Business Media: Dordrecht, The Netherlands, 2014; pp. 215–240.
15. Wulder, M.A.; Coops, N.C.; Hudak, A.T.; Morsdorf, F.; Nelson, R.; Newnham, G.; Vastaranta, M. Status and prospects for LiDAR remote sensing of forested ecosystems. *Can. J. Remote Sens.* **2013**, *39*, S1–S5. [[CrossRef](#)]
16. Boas, F. The Horizontal Plane of the Skull and the General Problem of the Comparison of Variable Forms. *Science* **1905**, *21*, 862–863. [[CrossRef](#)] [[PubMed](#)]
17. Von Neumann, J. Some matrix inequalities and metrization of matrix space. *Tomsk Univ. Rev.* **1937**, *1*, 286–300.
18. Claude, J. *Morphometrics with R*; Springer: New York, NY, USA, 2008; p. 316.
19. Slice, D.E. Geometric Morphometrics. *Annu. Rev. Anthropol.* **2007**, *36*, 261–281. [[CrossRef](#)]
20. Theobald, D.L. Likelihood and Empirical Bayes Superposition of Multiple Macromolecular Structures. In *Bayesian Methods in Structural Bioinformatics*; Hamelryck, T., Mardia, K., Ferkinghoff-Borg, J., Eds.; Springer: Berlin/Heidelberg, Germany, 2012; pp. 191–208.
21. Gonzalez, R.C.; Woods, R.E. *Digital Image Processing*, 3rd ed.; Prentice-Hall, Inc.: Upper Saddle River, NJ, USA, 2002; p. 793.
22. Ørka, H.O.; Gobakken, T.; Næsset, E.; Ene, L.; Lien, V. Simultaneously acquired airborne laser scanning and multispectral imagery for individual tree species identification. *Can. J. Remote Sens.* **2012**, *38*, 125–138. [[CrossRef](#)]
23. Baffetta, F.; Corona, P.; Fattorini, L. A matching procedure to improve k-NN estimation of forest attribute maps. *For. Ecol. Manag.* **2012**, *272*, 35–50. [[CrossRef](#)]
24. Gilichinsky, M.; Heiskanen, J.; Barth, A.; Wallerman, J.; Egberth, M.; Nilsson, M. Histogram matching for the calibration of kNN stem volume estimates. *Int. J. Remote Sens.* **2012**, *33*, 7117–7131. [[CrossRef](#)]
25. Vauhkonen, J.; Mehtätalo, L. Matching remotely sensed and field-measured tree size distributions. *Can. J. For. Res.* **2014**, *45*, 353–363. [[CrossRef](#)]
26. Xu, Q.; Hou, Z.; Maltamo, M.; Tokola, T. Calibration of area based diameter distribution with individual tree based diameter estimates using airborne laser scanning. *ISPRS J. Photogramm. Remote Sens.* **2014**, *93*, 65–75. [[CrossRef](#)]
27. Nyström, M.; Holmgren, J.; Olsson, H. Change detection of mountain birch using multi-temporal ALS point clouds. *Remote Sens. Lett.* **2013**, *4*, 190–199. [[CrossRef](#)]
28. Hauglin, M.; Ørka, H. Discriminating between Native Norway Spruce and Invasive Sitka Spruce—A Comparison of Multitemporal Landsat 8 Imagery, Aerial Images and Airborne Laser Scanner Data. *Remote Sens.* **2016**, *8*, 363. [[CrossRef](#)]
29. Javad Positioning Systems. *Pinnacle User's Manual*; Knowledge Base: San Jose, CA, USA, 1999.
30. Braastad, H. Volume tables for birch. *Rep. Nor. For. Res. Inst.* **1966**, *21*, 265–365. (In Norwegian)

31. Brantseg, A. Volume functions and tables for Scots pine, South Norway. *Rep. Nor. For. Res. Inst.* **1967**, *22*, 689–739. (In Norwegian)
32. Vestjordet, E. Functions and tables for volume of standing trees, Norway spruce. *Rep. Nor. For. Res. Inst.* **1967**, *22*, 543–574. (In Norwegian)
33. Bauger, E. Tree volume functions and tables. Scots pine, Norway spruce and Sitka spruce in western Norway. *Rapp. Skogforsk* **1995**, *16*, 26. (In Norwegian)
34. Fitje, A.; Vestjordet, E. Stand height curves and new tariff tables for Norway spruce. *Rep. Nor. For. Res. Inst.* **1977**, *34*, 23–68. (In Norwegian)
35. Axelsson, P. DEM generation from laser scanner data using adaptive TIN models. *Int. Arch. Photogramm. Remote Sens.* **2000**, *33*, 110–117.
36. Soinininen, A. *TerraScan User's Guide*; Helsinki Finland: Terrasolid Oy, Finland, 2016.
37. Gobakken, T.; Næsset, E.; Nelson, R.; Bollandsås, O.M.; Gregoire, T.G.; Ståhl, G.; Holm, S.; Ørka, H.O.; Astrup, R. Estimating biomass in Hedmark County, Norway using national forest inventory field plots and airborne laser scanning. *Remote Sens. Environ.* **2012**, *123*, 443–456. [[CrossRef](#)]
38. Dryden, I.L.; Mardia, K.V. *Statistical Shape Analysis: With Applications in R*, 2nd ed.; John Wiley and Sons: Hoboken, NJ, USA, 2016; p. 496. ISBN 978-0-470-69962-1.
39. Borg, I.; Groenen, P.J.F. *Modern Multidimensional Scaling: Theory and Applications*, 2nd ed.; Springer: New York, NY, USA, 2005; p. 614. ISBN 0-387-25150-2.
40. R Development Core Team. *R: A Language and Environment for Statistical Computing*; R Foundation for Statistical Computing: Vienna, Austria, 2016.
41. Martin, A.D.; Quinn, K.M.; Park, J.H. MCMCpack: Markov Chain Monte Carlo in R. *J. Stat. Softw.* **2011**, *42*, 1–21. [[CrossRef](#)]
42. Oksanen, J.; Guillaume Blanchet, F.; Friendly, M.; Kindt, R.; Legendre, P.; McGlenn, D.; Minchin, P.R.; O'Hara, R.B.; Simpson, G.L.; Solymos, P.; et al. *Vegan: Community Ecology Package*. R Package Version 2.4-2. 2017. Available online: <https://CRAN.R-project.org/package=vegan> (accessed on 4 October 2017).
43. Borchers, H.W. *Pracma: Practical Numerical Math Functions*. R Package Version 1.9.9. 2017. Available online: <https://CRAN.R-project.org/package=pracma> (accessed on 4 October 2017).
44. Hansen, E.H.; Gobakken, T.; Bollandsås, O.M.; Zahabu, E.; Næsset, E. Modeling Aboveground Biomass in Dense Tropical Submontane Rainforest Using Airborne Laser Scanner Data. *Remote Sens.* **2015**, *7*, 788–807. [[CrossRef](#)]
45. Næsset, E.; Gobakken, T. Estimation of above- and below-ground biomass across regions of the boreal forest zone using airborne laser. *Remote Sens. Environ.* **2008**, *112*, 3079–3090. [[CrossRef](#)]
46. Næsset, E. Practical large-scale forest stand inventory using a small-footprint airborne scanning laser. *Scand. J. For. Res.* **2004**, *19*, 164–179. [[CrossRef](#)]
47. Næsset, E.; Gobakken, T.; Bollandsås, O.M.; Gregoire, T.G.; Nelson, R.; Ståhl, G. Comparison of precision of biomass estimates in regional field sample surveys and airborne LiDAR-assisted surveys in Hedmark County, Norway. *Remote Sens. Environ.* **2013**, *130*, 108–120. [[CrossRef](#)]
48. Sugiura, N. Further analysts of the data by Akaike's information criterion and the finite corrections. *Commun. Stat. Theory Methods* **1978**, *7*, 13–26. [[CrossRef](#)]
49. Sestelo, M.; Villanueva, N.M.; Roca-Pardinas, J. Selecting Variables in Regression Models. R package version 2.1.0. 2015. Available online: <https://cran.r-project.org/web/packages/FWDselect/index.html> (accessed on 1 September 2016).
50. Zuur, A.F.; Ieno, E.N.; Walker, N.J.; Saveliev, A.A.; Smith, G.M. *Mixed Effects Models in Extensions in Ecology with R. Statistics for Biology and Health*; Springer: New York, NY, USA, 2009; p. 574. ISBN 978-0-387-87458-6.
51. Calcagno, V. *Glmulti: Model Selection and Multimodel Inference Made Easy*. R Package Version 1.0.7. 2013. Available online: <https://cran.r-project.org/web/packages/glmulti/index.html> (accessed on 1 September 2016).
52. Chai, T.; Draxler, R.R. Root mean square error (RMSE) or mean absolute error (MAE)?—Arguments against avoiding RMSE in the literature. *Geosci. Model Dev.* **2014**, *7*, 1247–1250. [[CrossRef](#)]
53. Asner, G.P. Tropical forest carbon assessment: Integrating satellite and airborne mapping approaches. *Environ. Res. Lett.* **2009**, *4*, 1–11. [[CrossRef](#)]

54. Packalen, P.; Strunk, J.L.; Pitkanen, J.A.; Temesgen, H.; Maltamo, M. Edge-Tree Correction for Predicting Forest Inventory Attributes Using Area-Based Approach with Airborne Laser Scanning. *IEEE J. Sel. Top. Appl. Earth Obs. Remote Sens.* **2015**, *8*, 1274–1280. [[CrossRef](#)]
55. Breidenbach, J.; Næsset, E.; Lien, V.; Gobakken, T.; Solberg, S. Prediction of species specific forest inventory attributes using a nonparametric semi-individual tree crown approach based on fused airborne laser scanning and multispectral data. *Remote Sens. Environ.* **2010**, *114*, 911–924. [[CrossRef](#)]
56. Bohlin, J.; Wallerman, J.; Fransson, J.E.S. Forest variable estimation using photogrammetric matching of digital aerial images in combination with a high-resolution DEM. *Scand. J. For. Res.* **2012**, *27*, 692–699. [[CrossRef](#)]
57. Gobakken, T.; Bollandsås, O.M.; Næsset, E. Comparing biophysical forest characteristics estimated from photogrammetric matching of aerial images and airborne laser scanning data. *Scand. J. For. Res.* **2015**, *30*, 73–86. [[CrossRef](#)]
58. Awadallah, M.S.; Abbott, A.L.; Thomas, V.A.; Wynne, R.H.; Nelson, R.F. Estimating Forest Canopy Height using Photon-counting Laser Altimetry. In Proceedings of the Silvilaser 2013: 13th International Conference on LiDAR Applications for Assessing Forest Ecosystems, Beijing, China, 9–11 October 2013; p. 8.
59. Swatantran, A.; Tang, H.; Barrett, T.; DeCola, P.; Dubayah, R. Rapid, High-Resolution Forest Structure and Terrain Mapping Over Large Areas using Single Photon Lidar. *Sci. Rep.* **2016**, *6*, 1–12. [[CrossRef](#)] [[PubMed](#)]



© 2017 by the authors. Licensee MDPI, Basel, Switzerland. This article is an open access article distributed under the terms and conditions of the Creative Commons Attribution (CC BY) license (<http://creativecommons.org/licenses/by/4.0/>).